

Go and return propagation of biphotons in fiber and polarization entanglement

G. Brida, M. Genovese, L. A. Krivitsky

Istituto Nazionale di Ricerca Metrologica, Strada delle Cacce 91, 10135 Torino, Italy

M. V. Chekhova

Department of Physics, M.V.Lomonosov Moscow State University, Leninskie Gory, 119992 Moscow, Russia

E. Predazzi

Dip. Fisica Teorica Univ. Torino and INFN, via P. Giuria 1, 10125 Torino, Italy

Propagation of entangled photons in optical fiber is one of the fundamental issues for realizing quantum communication protocols. When entanglement in polarization is considered, arises the problem of compensating for the fiber effect on photons polarization. In this paper we demonstrate an effective solution where a Faraday mirror allows to cancel undesired effects of polarization drift in fiber. This technique is applied to a protocol for generating Bell states by a narrow temporal selection of the second-order intensity correlation function.

PACS numbers: 42.50.Dv, 03.67.Hk, 42.62.Eh

I. INTRODUCTION

Transmission of photons in optical fibers is a fundamental tool both for realizing quantum communication protocols [1] and for experiments addressed to test foundations of quantum mechanics [2]. For example, long-distance quantum key distribution protocols in fiber have been realized by exploiting interferometric schemes [3] up to 100 km.

When quantum communication protocols are realized with photon states encoded in polarization some general difficulty must be considered connected with the transmission of photons through optical fibers. The photons propagating in fibers experience random polarization transformations due to the fluctuations of the fiber birefringence. These fluctuations are caused by mechanical, acoustic and thermal stresses in the fiber. Since it is impossible to completely isolate the fiber from the external disturbance the problem of an effective compensation for the polarization drift becomes a crucial issue. For instance a Quantum Key Distribution (QKD) protocol with polarization-entangled states produced via a type-II parametric down conversion (PDC) source was realized between a bank and the Vienna city hall by using a 1.45 km optical fiber [4]. Another example is a QKD network, involving also fiber propagation of polarization entangled photons, built among several research institutes in Boston [5]. In these examples a correction for the fiber effect on polarization was introduced, moreover, this correction was tuned in time quite often due to the instability of the fiber. A similar correction has also been needed in experiments on the study of the interference structure in the second-order intensity correlation function [6, 7], visualized due to the spreading of the two-photon wave packet propagating through an optical fibre.

However, in experiments where the photon travels along the fiber in both directions (there and back), a more efficient scheme can be adopted. Indeed in [8] it was shown that a Faraday cell followed by a mirror acts as a temporal inversion matrix, $\begin{bmatrix} 0 & -1 \\ -1 & 0 \end{bmatrix}$ in the Jones formalism. Thus the effect of the fiber on the polarization is reversed and cancels out when the photons are reflected back to the fiber by a Faraday mirror. Let us notice that a similar transformation cannot be obtained with retardation plates and mirrors. An experiment with polarized light proved the viability of the scheme [9], which was later successfully applied to realize an interferometer [10]. In particular, such configuration can find a very useful application in "go and return" quantum communication protocols as the ones of Ref. [11].

In this paper we discuss the application of the Faraday mirror to observe quantum interference in the shape of the second-order correlation function where bipartite polarization entangled states are produced in a type-II PDC process.

II. THEORY

We investigate degenerate type-II PDC emission in the collinear direction to the pump beam (the photons of a pair have the same frequencies and orthogonal polarizations). In low gain regime, neglecting higher orders, the state vector of the PDC light can be represented as a superposition of the vacuum state and the two-photon state given by an integral over the spectrum

$$|\Psi\rangle = |vac\rangle + \int d\Omega F(\Omega) [a_H^\dagger(\omega_0 + \Omega) a_V^\dagger(\omega_0 - \Omega) e^{i\Omega\tau_0} + a_V^\dagger(\omega_0 + \Omega) a_H^\dagger(\omega_0 - \Omega) e^{-i\Omega\tau_0}] |vac\rangle, \quad (1)$$

with $\omega_0 = \omega_p/2$, ω_p being the pump frequency, and a_H^\dagger and a_V^\dagger being the photon creation operators in the horizontal and vertical polarization modes (denoted by H, V). The phase factor $e^{\pm i\Omega\tau_0}$ is defined by the average temporal delay between orthogonally polarized photons, where $\tau_0 = DL/2$, $D \equiv 1/u_V - 1/u_H$ being the difference of the inverse group velocities and L the length of the crystal. The spectral and temporal properties of two-photon light are described by the two-photon spectral amplitude $F(\Omega)$ which establishes the natural bandwidth of PDC. The second-order correlation function $G^{(2)}(\tau)$ (the observable typically measured in experiments with PDC) is given by the square modulus of the Fourier transform of $F(\Omega)$, which is called the biphoton amplitude [12],

$$G^{(2)}(\tau) \propto |F(\tau)|^2 = \left| \int d\Omega F(\Omega) \exp(i\Omega\tau) \right|^2. \quad (2)$$

When the state (1) is transmitted through an optical fiber with Group-Velocity Dispersion (GVD), as it has been shown in [13], a Fourier transformation is performed over the biphoton amplitude $F(\tau)$. Thus, this takes the shape of the two-photon spectral amplitude $F(\Omega)$. This effect has a clear analogue with the propagation of a short optical pulse in a GVD media and results in changing the shape of the pulse to the shape of its spectrum. As it was shown in [6], $G^{(2)}(\tau)$ shows an interference structure depending on the polarization selection performed over each photon of a pair. Namely, if after dividing the two photons on a 50/50 beamsplitter [14], they are registered either with the same orientations of polarization filters set at 45° to initial basis or with the orthogonal orientations of the polarization filters set at 45° and -45° , $G^{(2)}(\tau)$ takes the form

$$\begin{aligned} G_+^{(2)}(\tau) &\sim \frac{\sin^2(\tau/\tau_f) \cos^2(\tau/\tau_f)}{(\tau/\tau_f)^2}, \\ G_-^{(2)}(\tau) &\sim \frac{\sin^4(\tau/\tau_f)}{(\tau/\tau_f)^2}. \end{aligned} \quad (3)$$

In Eq.3 $G_+^{(2)}$ and $G_-^{(2)}$ correspond, respectively, to parallel (both at 45°) and orthogonal (one at 45° and another one at -45°) orientations of the polarization filters in the output ports of the beamsplitter. $\tau_f \equiv 2k''z/\tau_0$ is the typical width of the correlation function after the fibre [15], z being the length of the crystal and k'' the second derivative of the fibre dispersion law $k(\omega)$.

Now let us focus on the problem of polarization drift in the fiber and its influence on the polarization entanglement. Upon passing the fiber, the initial polarization state of each photon (horizontal or vertical) is transformed from the equator of the Poincaré sphere to some arbitrary point on its surface [16]. This unitary transformation can be modelled as a polarization rotation by means of a retardation plate with an arbitrary optical thickness δ and orientation of the optical axis to initial basis α [17]. Applying the Jones formalism to the transformation of the creation operators in (1) it can be shown that for a given parameters of the retardation plate δ and α , the shape of $G_+^{(2)}$ and $G_-^{(2)}$ change from (3) to

$$\begin{aligned} G_+^{(2)}(\tau) &\sim [\cos^2 \delta (1 + \sin^2 \delta) + \sin^4 \delta \cos^2(4\alpha)] \frac{\sin^2(\tau/\tau_f) \cos^2(\tau/\tau_f)}{(\tau/\tau_f)^2}, \\ G_-^{(2)}(\tau) &\sim [\sin^2(4\alpha) \sin^4 \delta \cos^2(\tau/\tau_f) + \sin^2(\tau/\tau_f)] \frac{\sin^2(\tau/\tau_f)}{(\tau/\tau_f)^2}. \end{aligned} \quad (4)$$

The general dependence of G_\pm on the parameters δ and α is shown in Fig.1. From this one can prove the complexity of the variation of the interference pattern as a function of α and δ .

Let us now focus on the generation of Bell states. As it was shown in [6] a Bell state can be produced by performing a narrow temporal post-selection in the shape of $G^{(2)}(\tau)$. This can be realized, for instance, by analyzing the $G^{(2)}(\tau)$ distribution with a Time to Amplitude Converter (TAC) and a Multi Channel Analyzer (MCA), in which only specific channels are selected. When one selects the central part of $G^{(2)}(\tau)$ corresponding to zero delay, i.e. $\tau = 0$ (which is equivalent to the selection of $\Omega = 0$ in the frequency domain), the state (1) becomes the polarization-spatial entangled Bell state: $|\psi^+\rangle = \{a_{H1}^\dagger a_{V2}^\dagger + a_{V1}^\dagger a_{H2}^\dagger\} |vac\rangle$, where $a_{\sigma i}^\dagger$ are photon creation operators in the horizontal and vertical polarization modes (denoted by $\sigma = H, V$) and in two spatial modes of the beamsplitter (denoted by $i = 1, 2$). Being a pure maximally entangled state, $|\psi^+\rangle$ manifests 100% visibility of polarization interference [18]. However, if we

consider the transformation of $|\psi^+\rangle$ in fiber, for instance modelled for the sake of simplicity by a Half Wave Plate (HWP) with variable orientation α , then, as one can see from Fig.2 (a section of Fig.1), the visibility of polarization interference at $\tau = 0$ changes from 100% for the case when $\alpha = 0^\circ$ (which is equivalent to the absence of rotation) to zero when $\alpha = 11, 25^\circ$. Moreover, at $\alpha = 22, 5^\circ$ the two-photon state becomes an eigen-state of the measurement basis (photons of the pair are polarized at 45° and -45°) and the interference structure is completely erased. Thus, even considering the simplest model of polarization rotation produced by the fiber, this leads to spoiling the polarization interference and to erasing the polarization entanglement.

This problem has motivated our choice of applying a Faraday mirror to compensate for these effects. Moreover, taking into account a wide natural bandwidth of PDC spectra (typically of the order of ten nanometers) it is worth mentioning that the implementation of an appropriate Faraday mirror allows also to correct for the effects related to frequency dependence of the effective birefringence in the fiber on the wavelength.

On the other hand, if the selected time interval corresponds to $\tau = \pm\pi\tau_f/2$, the relative phase between the two components of the state (1) becomes equal to π and the biphoton state represents the polarization-frequency singlet Bell state: $|\psi^-\rangle = \{a_{H1}^\dagger(\omega_1)a_{V2}^\dagger(\omega_2) - a_{V1}^\dagger(\omega_1)a_{H2}^\dagger(\omega_2)\}|vac\rangle$, where the two frequency modes are $\omega_1 = \omega_0 + \pi/2\tau_0$; $\omega_2 = \omega_0 - \pi/2\tau_0$. As one can see from (4), the visibility of polarization interference in this case remains 100% and does not depend on the polarization rotation induced by the fiber. This confirms a noticeable property of the singlet Bell state, namely, its invariance with respect to any polarization transformation. Therefore for the case of the selection of $|\psi^-\rangle$ no compensation for the polarization drift is needed at all [19].

III. EXPERIMENTAL SET-UP AND DATA

In our set-up, see Fig.3, biphoton pairs were generated via spontaneous parametric down-conversion by pumping a type-II 0.5 mm BBO crystal with a 0.5 Watt Ar^+ cw laser beam at the wavelength 351 nm in the collinear frequency-degenerate regime. After the crystal, the pump laser beam was eliminated by a 95% reflecting UV mirror and the PDC radiation was coupled into a 240 m long single-mode non polarization maintaining fibre with field mode diameter $= 4\mu\text{m}$ by a 20x microscope objective lens placed at the distance of 50 cm. This scheme provided imaging of the pump beam waist onto the fibre input with the magnification 1:40. For the efficient use of the pump beam, the pump was focused into the crystal using a UV-lens with the focal length of 30 cm. The resulting beam waist diameter, $120\mu\text{m}$, was small enough to be coupled with the fibre core diameter, but still sufficiently large not to influence the PDC angular spectrum.

After the first passage through the fiber, biphotons were addressed back by a free-space Faraday mirror, consisting of a Faraday rotator and a high-reflection mirror. In this way the polarization effects of the fiber were compensated. Then, after having crossed the crystal, the photons passed the UV mirror needed for the injection of the pump beam into the crystal and reached the 50/50 beam splitter preceding the detection apparatuses, consisting of polarizers and two avalanche photodiodes. The photocount pulses of the two detectors were sent to the START and STOP inputs of a TAC. The output of the TAC was finally addressed to a MCA, and the distribution of coincidences over the time interval between the photocounts of two detectors was observed at the MCA output.

The second-order intensity correlation function measured in the experiment for the case when both polarizers are parallel (set at 45°) and orthogonal (set at 45° and -45°) are presented in Fig.4. The results show a good agreement with the theoretical predictions (3). Here we would like to stress that the fiber was not placed in any isolation box or similar device so that it experienced the influence of heating in the lab, acoustic and mechanical stresses during all the acquisition time which exceeded two hours. Moreover, the fiber we used was unwound from the spool and did not have an isolation plastic core. We have checked that in a single-pass configuration under the same conditions the polarization effects of the fiber drift on a time scale of 5-7 minutes [21].

Thus our results demonstrate that a perfect stability of the setup in "go and return" configuration over polarization fluctuations introduced by the fibre can be achieved by using a Faraday mirror.

The visibility of polarization interference at zero time delay measured in the experiment and calculated from Fig.4 was 72% (after background subtraction). This reduction of the measured visibility with respect to theoretical predictions is explained by the length of the fibre, insufficient to make the spreading of $G^2(\tau)$ significantly larger than the time resolution of the set-up. Indeed, the fibre was chosen to be only $2 \times 240\text{m}$ long in order to avoid high losses of the signal (about 12dB/km at 702 nm). A more detailed discussion on the influence of the fiber length on the visibility of polarization interference can be found in [7].

IV. CONCLUSIONS

In conclusion we demonstrated an application of the "go and return" scheme for generating entangled states with the help of the spreading of the second-order intensity correlation function. We have shown that the implementation of the Faraday mirror allows to compensate for the polarization drift in the fiber, which is crucial for obtaining polarization entangled Bell states. Our experimental data verifies the stability of the scheme under the influence of external disturbances over the fiber.

V. ACKNOWLEDGEMENTS

This work was supported by MIUR (FIRB RBAU01L5AZ-002 and PRIN 2005023443-002), by Regione Piemonte (E14), and by "San Paolo foundation". Maria Chekhova also acknowledges the support of the Russian Foundation for Basic Research, grant no.06-02-16393.

We would like also to acknowledge Luca Giacone for his assistance in the realization of this experiment.

References

-
- [1] Gisin N. et al. 2002 *Rev. Mod. Phys.* **74** 145.
 - [2] Genovese M. 2005 *Phys. Rep.* **413** 319.
 - [3] Marcikic I. et al. *Preprint* quant-ph/0404124. Mo X. et al., quant-ph/0412023; Kimura T. et al. 2004 *Jpn. J. Appl. Phys.* **43** L1217; Hiskett P.A. et al. 2006 *New Journal of Phys.* **8** 193.
 - [4] Poppe A. et al. 2004 *Opt. Express* **12** 3865.
 - [5] C. Elliot et al., quant-ph 0503058.
 - [6] Brida G., Genovese M., Gramegna M., Krivitsky L.A. and Chekhova M.V. 2006 *Phys. Rev. Lett.* **96** 143601.
 - [7] Brida G., Genovese M., Krivitsky L.A. and Chekhova M.V. 2006 *Preprint* quant-ph/0607137.
 - [8] Martinelli M. 1992 *Journ. Mod. Opt.* **39** 451
 - [9] Martinelli M. 1989 *Opt. Comm.* **72** 341
 - [10] Breguet J. and Gisin N. 1995 *Opt. Lett.* **20** 1447.
 - [11] Boström K. *Preprint* quant-ph 0203064; Degiovanni I.P. et al. 2005 *Phys. Rev. A* **71**, 016302; Boström K. and Felbinger T. 2002 *Phys. Rev. Lett.* **89** 187902. Cere' A. et al. 2006 *Phys. Rev. Lett.* **96** 200501; Lucamarini M. and Mancini S. 2005 *Phys. Rev. Lett.* **94** 140501.
 - [12] Rubin M.H., Klyshko D.N., Shih Y.H., and Sergienko A.V. 1994 *Phys. Rev. A* **50** 5122.
 - [13] Valencia A., Chekhova M.V. , Trifonov A.S. , and Shih Y.H. 2002 *Phys. Rev. Lett.* **88** 183601.
 - [14] Here we only consider the case when two photons of the pair go into different ports of the beamsplitter.
 - [15] Krivitsky L.A. and Chekhova M.V. 2005 *JETP Lett.* **81**, 125.
 - [16] Chekhova M.V., Krivitsky L.A. , Kulik S.P., Maslennikov G.A. 2004 *Phys. Rev. A* **70** 053801.
 - [17] In following calculations we neglect the chromatic dispersion of the fiber i.e. the optical thickness δ is considered constant for all the spectrum of PDC.
 - [18] Here we define the visibility in the traditional way as the difference of coincidences measured in orthogonal bases divided by their sum.
 - [19] Zanardi P. and Rasetti M. 1997 *Phys. Rev. Lett.* **79** 3306; Kwiat P. et al. 2000 *Science* **290** 498.
 - [20] Benatti F. and Floreanini R. quant-ph 0607071.
 - [21] The strong coupling between fiber and environment and the polarization effects induced by this are the most important problem for quantum communication with polarization as qubit, on the other hand this coupling can be useful for studying properties of quantum channels as Complete Positivity [20] or decoherence control protocols.



FIG. 1: Variation with $t = \tau/\tau_f$ of G_+ (first 2 lines) and G_- (last 2 lines). For both G_+ and G_- , the first line is for α varying between 0 and $\pi/2$ with δ fixed at $\delta = \pi/6, \pi/4, \pi/3, \pi/2$. The second line corresponds to δ varying between 0 and $\pi/2$ with α fixed at $\alpha = \pi/6, \pi/4, \pi/3, \pi/2$.

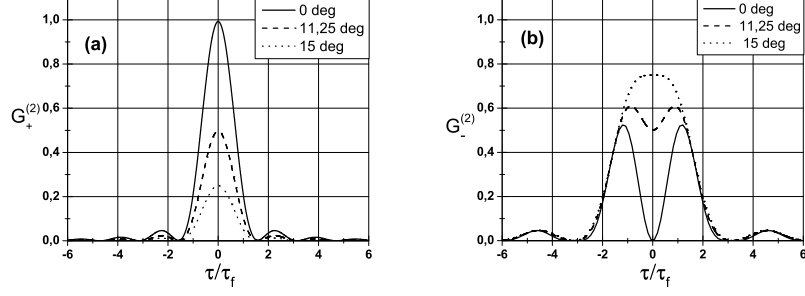


FIG. 2: The second order intensity correlation function for different orientations of the HWP acting on type II PDC state in frequency degenerate regime. $G_+^{(2)}$ corresponds to parallel orientations of polarization filters set to 45° (a); $G_-^{(2)}$ corresponds to orthogonal orientations of polarization filters set to 45° and -45° (b).

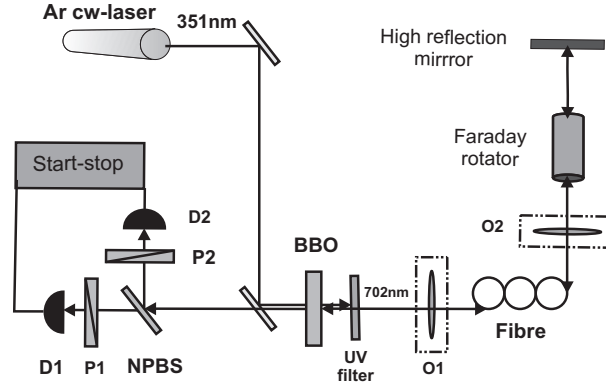


FIG. 3: The experimental setup. A cw Ar^+ laser at 351 nm pumps a type-II BBO crystal; O1, O2- microscope objectives; compensation for polarization drift in fibre is performed by free-space Faraday mirror, consisting of Faraday rotator and high-reflection mirror; NPBS - 50/50 nonpolarizing beamsplitter; P1 and P2- Glan prisms; D1, D2- avalanche photodiodes. The output of the Start-Stop scheme is analyzed by a multi-channel analyzer (MCA).

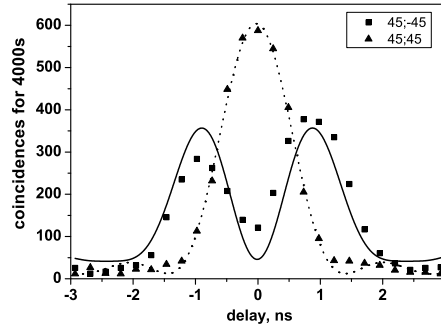


FIG. 4: Experimental dependence of the coincidence count rate on the time delay between two photons for two cases: both polarizers are parallel and set at 45° (triangles) and polarizers are orthogonal and set at 45° and -45° (squares). The dashed and solid curves represent the fit of experimental data for $45^\circ; 45^\circ$ and $45^\circ; -45^\circ$ configurations respectively.